Evolution of the solar wind proton temperature anisotropy from 0.3 to 2.5 AU

Lorenzo Matteini,[1,2] Simone Landi,[1] Petr Hellinger,[3] Filippo Pantellini,[2] Milan Maksimovic,[2] Marco Velli,[4,5] Bruce E. Goldstein,[4] and Eckart Marsch[6]

[1] We report an analysis of the proton temperature anisotropy evolution from 0.3 to 2.5 AU based on the Helios and Ulysses observations. With increasing distance the fast wind data show a path in the parameter space ($\beta_{\|p}$, $T_{\perp p}/T_{\|p}$). The first part of the trajectory is well described by an anticorrelation between the temperature anisotropy $T_{\perp p}/T_{\|p}$ and the proton parallel beta, while after 1 AU the evolution with distance in the parameter space changes and the data result in agreement with the constraints derived by a fire hose instability. The slow wind data show a more irregular behavior, and in general it is not possible to recover a single evolution path. However, on small temporal scale we find that different slow streams populate different regions of the parameter space, and this suggests that when considering single streams also the slow wind follows some possible evolution path. **Citation:** Matteini, L., S. Landi, P. Hellinger, F. Pantellini, M. Maksimovic, M. Velli, B. E. Goldstein, and E. Marsch (2007), Evolution of the solar wind proton temperature anisotropy from 0.3 to 2.5 AU, *Geophys. Res. Lett.*, *34*, L20105, doi:10.1029/2007GL030920.

1. Introduction

[2] Direct observations of the solar wind plasma have suggested that at 1 AU the proton velocity distribution functions are constrained by the wave-particle interaction deriving from plasma instabilities [it *Kasper et al.*, 2002; *Hellinger et al.*, 2006]. It is an open question if the same behavior can be observed also at other distances. The main instabilities driven by a proton temperature anisotropy are the mirror and the proton-cyclotron instabilities in the case that the perpendicular (with respect to the ambient magnetic field) proton temperature is greater than the parallel temperature ($T_{\perp p} > T_{\|p}$) and the parallel and the oblique fire hose instabilities for $T_{\|p} > T_{\perp p}$. The main parameters are the proton temperature anisotropy $T_{\perp p}/T_{\|p}$ and parallel beta $\beta_{\|p}$. In the case of an ideal adiabatic (i.e., CGL [from *Chew et al.*, 1956] or double-adiabatic) expansion, with a constant flow velocity and in a radial magnetic field, these parameters would change with the radial distance as:

$$\frac{T_{\perp p}}{T_{\|p}} \propto r^{-2} \quad \text{and} \quad \beta_{\|p} \propto r^{2}. \quad (1)$$

This means that even an initially isotropic low beta plasma, which is stable with respect the cited instabilities, can become unstable just because of the changes driven by the radial expansion in the system. Even if the adiabatic prediction of (1) does not apply to the real solar wind, where it is known that the adiabatic invariants are not conserved, a perpendicular cooling driving the fast wind from $T_{\perp p} > T_{\|p}$ at 0.3 AU to $T_{\perp p} \simeq T_{\|p}$ at 1 AU is observed [*Marsch et al.*, 1982]. In terms of the instability parameters *Marsch et al.* [2004] have found for the core part of the proton distribution in the fast wind the anticorrelation:

$$\frac{T_{\perp p}}{T_{\|p}} \sim \frac{a}{\beta_{\|p}^{b}}, \quad (2)$$

with $b \simeq 0.55$ and $a \simeq 1.16$. As the parallel beta increases with distance, if a relation like (2) remains valid all along the expansion, the plasma is predicted to approach after a certain distance the fire hose unstable regions. Numerical simulations [*Hellinger et al.*, 2003; *Matteini et al.*, 2006] predict that the anticorrelation between anisotropy and $\beta_{\|p}$ should then be broken with the distance, and for $\beta_{\|p} \simeq 1$ the solar wind is found to expand along a marginal stability path which corresponds to the equilibrium between the expansion and the fire hose saturation. The purpose of this letter is to check this behavior which is agreement with the observations at 1 AU on a larger range of distances. *Marsch et al.* [2006] have reported a study of Helios data on the range 0.3–1 AU finding for the global solar wind (without distinction between fast and slow) a statistical approach to the fire hose instability region with the distance. Here we extend this work using Ulysses data and we investigate the anisotropy evolution of the proton distribution functions from 0.3 AU to 2.5 AU. The data are divided into fast and slow wind as these two solar wind regimes show different properties in terms of the instabilities parameters. The observational results are compared with the linear theory prediction for the instability threshold conditions. We computed the plasma properties including the effects of the presence of a small fraction of alpha particles. A parallel study on the electron properties between 0.3 and 3 AU, based on data from the same spacecrafts is also in preparation (Š. Štverák et al., Electron temperature

[1]Dipartimento di Astronomia e Scienza dello Spazio, Università degli Studi di Firenze, Florence, Italy.
[2]Lesia, Observatoire de Paris, Paris, France.
[3]Institute of Atmospheric Physics, Academy of Sciences of Czech Republic, Prague, Czech Republic.
[4]Jet Propulsion Laboratory, Pasadena, California, USA.
[5]On leave from Dipartimento di Astronomia e Scienza dello Spazio, Università degli Studi di Firenze, Florence, Italy.
[6]Max-Planck-Institut für Sonnensystemforschung, Katlenburg-Lindau, Germany.
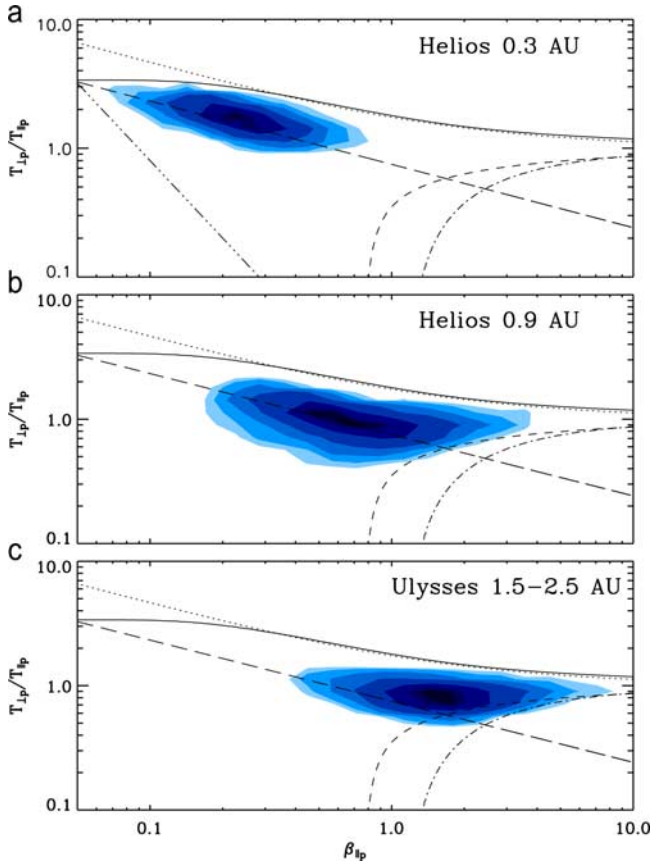
Figure 1. Fast wind data: Histograms refer to observations at (a) 0.3, (b) 0.8–0.9, and (c) 1.5–2.5 AU. In each panel we report the instability threshold conditions for the ion-cyclotron (solid), the mirror (dotted), the parallel (dashed), and the oblique (dash-dotted) fire hose instabilities. In Figure 1a the dash-dot-dot-dotted straight line refers to the CGL adiabatic prediction (1). In all panels the long dashed line shows the best fit of the anticorrelation (2) (computed for $\beta_{\|p} < 0.7$ data).

anisotropy constraints in the solar wind, submitted to *Journal of Geophysical Research*, 2007).

2. Data Analysis

[3] We report an analysis of the data from the space missions Helios (1 and 2) and Ulysses. Helios explored in the ecliptic plane the region from 0.3 to 1 AU, while Ulysses having an orbit external to the Earth and perpendicular to the ecliptic plane, explores the region from 1.3 to 5 AU. The use of combined data these missions then allows us to make a global study of the solar wind properties over an important distance range and enable the possibility of the analysis of radial evolution profiles [e.g., *Maksimovic et al.*, 2005]. The Helios data are analyzed following *Marsch et al.* [1982] and no assumptions about the shape of the particle distribution are made. For the Ulysses data we used the analysis algorithm of *Neugebauer et al.* [2001]. This procedure for the extraction of ion velocity distributions measured by the SWOOPS instrument has been used before

for statistical studies of the wave-particle interaction signatures in Ulysses observations [*Gary et al.*, 2002]; however the Ulysses data shown here, belonging to the north solar pole transit near the year 2001, have been analyzed for the first time with this procedure.

[4] Other works have pointed out the role of the proton core temperature anisotropy [*Marsch et al.*, 2004, 2006]; in our analysis we take into account the global proton distribution as all the velocities can contribute to the wave-particle interaction, and so we prefer to use here the total proton temperatures.

2.1. Fast Wind Data

[5] For the fast wind analysis ($v > 600$ km/s) we used the following data sets: a selection of the fast wind intervals measured during the first 30 days of year 1975 when Helios 1 was between 0.8 and 1 AU; the days 105–109 of year 1976 when Helios 2 was at 0.3 AU and measured a continuous flow of fast wind; the Ulysses north pole transit from July to December 2001, concerning distances from 1.5 to 2.5 AU and corresponding to a heliolatitude excursion from 40 to 80 degrees. We have selected data from these three different distance ranges in order to emphasize the temperature anisotropy evolution as a function of the heliocentric distance.

[6] In Figure 1 we report the histograms of the observational counts of ($\beta_{\|p}$, $T_{\perp p}/T_{\|p}$) normalized to the maximum of the distribution. The three panels refer to 0.3 AU (Figure 1a), 0.9 AU (Figure 1b) and 1.5–2.5 AU (Figure 1c). In each panel we report, following *Hellinger et al.* [2006], the marginal stability conditions for the proton-cyclotron (solid) and mirror (dotted) instabilities which can develop in the case $T_{\perp p} > T_{\|p}$ and for the parallel (dashed) and oblique (dash-dotted) fire hose instabilities which can take place when $T_{\|p} > T_{\perp p}$. The marginal stability conditions are chosen as the $\gamma_m = 10^{-3}\ \Omega_{cp}$ level as computed in the linear theory approximation, where γ_m is the maximum instability growth rate for a given value of ($\beta_{\|p}$, $T_{\perp p}/T_{\|p}$), and Ω_{cp} is the proton cyclotron frequency.

[7] The linear theory is here computed in the presence of alpha particles, fixing their properties (see next paragraph). This gives a more realistic description of the solar wind plasma where the alpha particles are not negligible. However other parameters, such as the alpha or the proton to alpha ratio temperature anisotropy, can change the instability regions, as well as the electron properties [e.g., *Dasso et al.*, 2003]. Also the presence of an alpha/proton velocity drift, which is a source of free energy for beam-type instabilities, can play a role on the dynamic of the instabilities driven by a proton temperature anisotropy [*Hellinger and Trávníček*, 2005, 2006]. Finally, from numerical simulations, *Araneda and Gomberoff* [2004] have shown that the presence of large amplitude waves can change the growth rates obtained from linear theory. Our choice of parameters is so not complete, but is an improvement of the usual assumption of an electron-proton plasma.

[8] The plasma parameters of our calculation are: $n_\alpha/n_e = 0.05$, $T_{\|p} = T_{\|\alpha}$, $T_{\perp\alpha}/T_{\|\alpha} = T_{\perp p}/T_{\|p}$; though the solar wind parameters usually have minor ion temperatures larger than the proton temperature, for alphas typically a factor of 4, this does not produce important changes in the qualitative picture shown in Figure 1. Electrons are taken to be
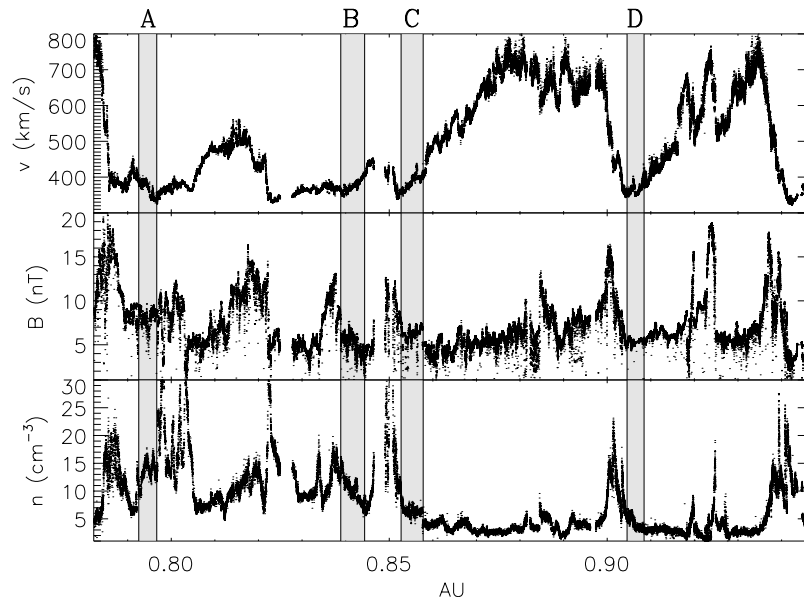
Figure 2. Helios measurements of (top) wind velocity, (middle) magnetic field, and (bottom) density. The grey regions encode the slow wind samples used in Figure 3.

isotropic and $\beta_e = 1$; protons are bi-Maxwellian and no drift is present between species. Finally, note that due to the presence of alpha particles the stability condition is computed here requiring the plasma to be stable with respect both proton and alpha species (see *Hellinger and Trávníček* [2005] for details).

[9] Comparing Figures 1a–1c, the data clearly show an evolution path in the parameter space. This path can be divided in two phases; the first from 0.3 to 0.9 AU suggests that the wind expands following an anticorrelation between proton parallel plasma beta and temperature anisotropy. The long-dashed line represents the best fit of relation (2) with $b \simeq 0.45$ and $a \simeq 1$; this has been computed taking into account data with $\beta_{\|p} < 0.7$ (the fire hose instability is predicted to play a role for $\beta_{\|p} > 0.7$) and results in good agreement with the values found by *Marsch et al.* [2004] for the distribution function core. The slope of the trajectory during this phase is less steep than the adiabatic CGL case (dash-double-dotted line in Figure 1a), meaning that during this part of the expansion a mechanism of perpendicular heating (and also parallel cooling [*Hu et al.*, 1997]) is at work.

[10] Also, for our choice of the alpha parameters, at 0.3 AU (Figure 1a) the observations are compatible with the proton-cyclotron instability constraints. Note that in general observations are not compatible with the proton-cyclotron threshold based on an electron-proton plasma [*Marsch et al.*, 2004; *Hellinger et al.*, 2006].

[11] With increasing distance the wind approaches the fire hose unstable regions and at 1 AU the trajectory changes (note in Figure 1b the change in the slope of the data distribution for $\beta_{\|p} \sim 0.8$–0.9); Ulysses data for greater distances (1.5–2.5 AU, Figure 1c) confirm this behavior. In this second phase of the expansion the plasma is not characterized any more by an increasing anisotropy $T_{\|p} > T_{\perp p}$ and the proton distribution functions follow a path which is in good agreement with the marginal stability path of a fire hose instability.

2.2. Slow Wind Data

[12] As shown by the WIND observations at 1 AU [*Kasper et al.*, 2002; *Hellinger et al.*, 2006] the slow wind ($v < 500$ km/s) populates a large part of the stable region of the parameter space; a global study of Ulysses slow wind data (not shown here) confirms in fact an analogous picture. Our analysis also supports the idea that the proton distribution functions in the slow wind statistically approach the fire hose unstable regions with the radial distance, as found by *Marsch et al.* [2006] for the Helios data only. As a consequence of their dispersion in the parameter space, the slow wind data do not show a single evolution path, and a relation between $\beta_{\|p}$ and the proton temperature anisotropy as (2) can not be found. However, the data show temperature anisotropies which seem to be correlated on small temporal scales. As an example we show in Figure 2 the velocity, density and magnetic field profiles from a sample of Helios observations. We have selected 4 periods of slow wind with almost constant conditions, encoded in grey in the figure. Data which do not have quiet magnetic field and density conditions are indicative of a possible interaction between different streams; as this would introduce a supplementary change in the velocity distribution anisotropy, these kind of observations have not been taken into account. The properties of the four streams in terms of $(\beta_{\|p}, T_{\perp p}/T_{\|p})$ are reported in Figure 3 where for each period we show the distribution in the parameter space. It results that on the scale of single streams, also the slow wind shows some path: data from the same stream populate the same region of the parameter space. Then the strong irregularity of the slow wind, where the density, the magnetic field intensity and the temperature ratio can vary strongly from one stream to another, makes the observed distribution functions populate different parts of the param-
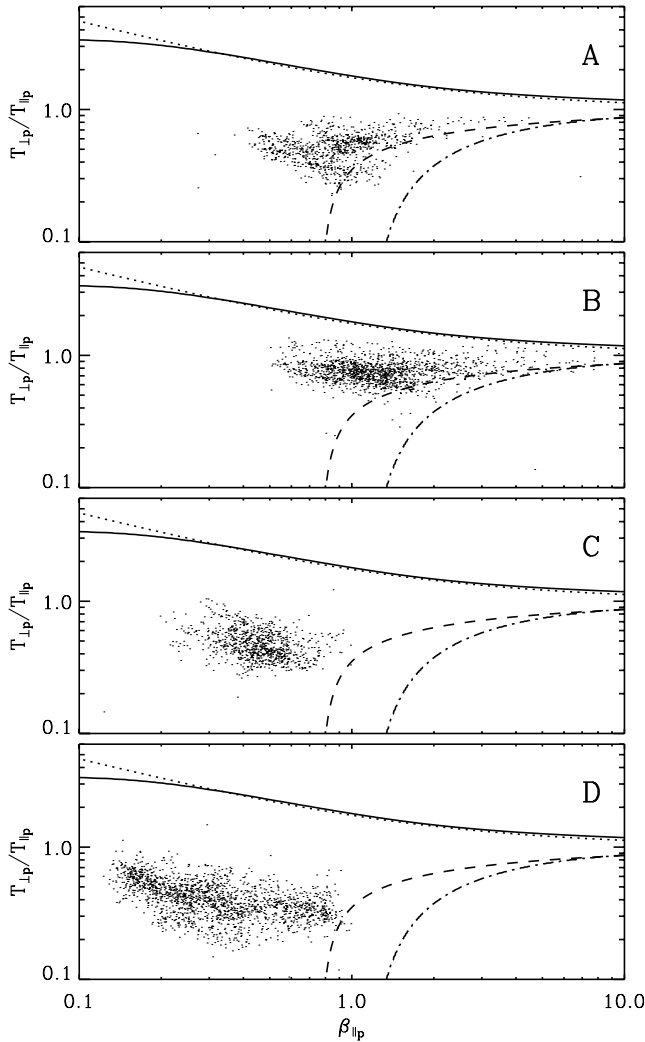
Figure 3. Temperature anisotropy and proton parallel plasma beta for different streams of slow solar wind (the letters A, B, C, and D encode the selected periods of Figure 2). As in Figure 1 the lines refer to the threshold condition ($\gamma_m = 10^{-3}\ \Omega_{cp}$) of plasma instabilities.

eter space, and it globally leads to a wide distribution of $\beta_{\|p}$ and anisotropy.

3. Conclusion

[13] We have presented a study of the proton temperature anisotropy from 0.3 to 2.5 AU. Both the slow and the fast wind are found to approach the fire hose instability regions with increasing distance. The fast wind data show a path in the parameter space moving from a low beta and $T_{\perp p} > T_{\|p}$ regime typical of 0.3 AU to $\beta_{\|p} \sim 1$ and $T_{\|p} > T_{\perp p}$ at 1 AU; this anticorrelation between parallel beta and anisotropy is in agreement with the result of *Marsch et al.* [2004]. After 1 AU the proton temperature anisotropy departs from the empirical relation observed by Helios between 0.3 and 1 AU and Ulysses data for further distances suggest that the macroscopic dynamic of the wind is dominated by the microscopic wave-particle activity of a fire hose instability. Even if the parallel fire hose instability is predicted dominant in the linear approximation (however as the measured

distribution functions can depart from a bi-Maxwellian some care must be use on comparing data with the theoretical predictions, which are derived for a bi-Maxwellian proton plasma), the data are closer to the constraints imposed by the oblique fire hose; the same behavior is found by *Hellinger et al.* [2006] in the slow wind. Simulations of the dynamical stabilization of the parallel fire hose instability in a frame of an expanding system [*Matteini et al.*, 2006] show that during the initial phase of the instability the expansion could be able to drive the system inside the unstable region enough to destabilize also the oblique fire hose. The solar wind dynamic should be then characterized by both types of fire hose instabilities. In this framework, preliminary results of 2D simulations indeed suggest a marginal stability path in qualitative agreement with the observations.

[14] In the slow wind it is not possible to recover a single evolution path with growing distance because, as shown, the slow wind irregularity makes different wind streams populate different regions of the parameter space. However the analysis of short samples shows the presence of possible evolution paths also in the slow wind; the different displacement of these paths in the parameter space depends probably on the variable initial conditions (in terms of proton beta and anisotropy) in the solar corona and/or on the variable collision rate, which characterize the slow wind plasma.

[15] A final comment on the observations of $T_{\perp p} > T_{\|p}$; the maximum of this anisotropy is measured at 0.3 AU and then it is relaxed with the distance. Our study does not indicate the origin of such an anisotropy; it remains an open question if relation (2) still describes the proton properties closer to the Sun. Theory of the ion-cyclotron heating predicts a limit on the proton anisotropy $T_{\perp p} > T_{\|p}$, and we have shown here that, for a choice of parameters, the presence of alpha particle in the plasma makes this limit compatible with the observations (solid line in Figure 1). It is however difficult to say if the data are constrained by the ion-cyclotron instability at previous distances. Concerning the expansion after 0.3 AU, signatures of a cyclotron heating are present in the proton distribution functions [*Tu and Marsch*, 2002; *Heuer and Marsch*, 2007], and this can explain the non-adiabatic evolution path of the fast wind in the parameter space.

[16] Finally also other mechanisms can change the evolution of the proton temperature anisotropy. The spiral form of the magnetic field could play a role in the change of the trajectory in the parameter space; however for a high latitude fast wind as the one measured by Ulysses used in this study, the change due to the magnetic field is negligible at the distance that we have analyzed. A study at greater distances where the contribution of the magnetic field on the anisotropy evolution could be important will be the subject of future studies, as well as the role of the collisions on regulating the temperature profiles.

References

Araneda, J. A., and L. Gomberoff (2004), Stabilization of right-hand polarized beam plasma instabilities due to a large-amplitude left-hand polar-

ized wave: A simulation study, *J. Geophys. Res.*, *109*, A01106, doi:10.1029/2003JA010189.

Chew, G. F., M. L. Goldberger, and F. E. Low (1956), The Boltzmann equation and the one-fluid hydromagnetic equations in the absence of particle collisions, *Proc. R. Soc. London*, *236*, 112–118.

Dasso, S., F. T. Gratton, and C. J. Farrugia (2003), A parametric study of the influence of ion and electron properties on the excitation of electromagnetic ion cyclotron waves in coronal mass ejections, *J. Geophys. Res.*, *108*(A4), 1149, doi:10.1029/2002JA009558.

Gary, S. P., B. E. Goldstein, and M. Neugebauer (2002), Signatures of wave-ion interactions in the solar wind: Ulysses observations, *J. Geophys. Res.*, *107*(A8), 1169, doi:10.1029/2001JA000269.

Hellinger, P., and P. Trávníček (2005), Magnetosheath compression: Role of characteristic compression time, alpha particle abundance, and alpha/proton relative velocity, *J. Geophys. Res.*, *110*, A04210, doi:10.1029/2004JA010687.

Hellinger, P., and P. Trávníček (2006), Parallel and oblique proton fire hose instabilities in the presence of alpha/proton drift: Hybrid simulations, *J. Geophys. Res.*, *111*, A01107, doi:10.1029/2005JA011318.

Hellinger, P., P. Trávníček, A. Mangeney, and R. Grappin (2003), Hybrid simulations of the expanding solar wind: Temperatures and drift velocities, *Geophys. Res. Lett.*, *30*(5), 1211, doi:10.1029/2002GL016409.

Hellinger, P., P. Trávníček, J. C. Kasper, and A. J. Lazarus (2006), Solar wind proton temperature anisotropy: Linear theory and WIND/SWE observations, *Geophys. Res. Lett.*, *33*, L09101, doi:10.1029/2006GL025925.

Heuer, M., and E. Marsch (2007), Diffusion plateaus in the velocity distributions of fast solar wind protons, *J. Geophys. Res.*, *112*, A03102, doi:10.1029/2006JA011979.

Hu, Y. Q., R. Esser, and S. R. Habbal (1997), A fast solar wind model with anisotropic proton temperature, *J. Geophys. Res.*, *102*, 14,661–14,676, doi:10.1029/97JA01040.

Kasper, J. C., A. J. Lazarus, and S. P. Gary (2002), Wind/SWE observations of firehose constraint on solar wind proton temperature anisotropy, *Geophys. Res. Lett.*, *29*(17), 1839, doi:10.1029/2002GL015128.

Maksimovic, M., et al. (2005), Radial evolution of the electron distribution functions in the fast solar wind between 0.3 and 1.5 AU, *J. Geophys. Res.*, *110*, A09104, doi:10.1029/2005JA011119.

Marsch, E., R. Schwenn, H. Rosenbauer, K.-H. Muehlhaeuser, W. Pilipp, and F. M. Neubauer (1982), Solar wind protons: Three-dimensional velocity distributions and derived plasma parameters measured between 0.3 and 1 AU, *J. Geophys. Res.*, *87*, 52–72.

Marsch, E., X.-Z. Ao, and C.-Y. Tu (2004), On the temperature anisotropy of the core part of the proton velocity distribution function in the solar wind, *J. Geophys. Res.*, *109*, A04102, doi:10.1029/2003JA010330.

Marsch, E., L. E. Zhao, and C.-Y. Tu (2006), Limits on the core temperature anisotropy of solar wind protons, *Ann. Geophys.*, *24*, 2057–2063.

Matteini, L., S. Landi, P. Hellinger, and M. Velli (2006), Parallel proton fire hose instability in the expanding solar wind: Hybrid simulations, *J. Geophys. Res.*, *111*, A10101, doi:10.1029/2006JA011667.

Neugebauer, M., B. E. Goldstein, D. Winterhalter, E. J. Smith, R. J. MacDowall, and S. P. Gary (2001), Ion distributions in large magnetic holes in the fast solar wind, *J. Geophys. Res.*, *106*, 5635–5648.

Tu, C.-Y., and E. Marsch (2002), Anisotropy regulation and plateau formation through pitch angle diffusion of solar wind protons in resonance with cyclotron waves, *J. Geophys. Res.*, *107*(A9), 1249, doi:10.1029/2001JA000150.

————————————

B. E. Goldstein, Jet Propulsion Laboratory, 4800 Oak Grove Drive, Pasadena, CA 91109, USA. (bruce.e.goldstein@jpl.nasa.gov)

P. Hellinger, Institute of Atmospheric Physics, Academy of Sciences of Czech Republic, Bocni II/1401, 14131 Prague 4, Czech Republic. (petr.hellinger@ufa.cas.cz)

M. Maksimovic and F. Pantellini, Lesia, Observatoire de Paris, F-92125 Meudon Cedex, France. (milan.maksimovic@obspm.fr; filippo.pantellini@obspm.fr)

E. Marsch, Max-Planck-Institut für Sonnensystemforschung, Max-Planck-Straße 2, D-37191 Katlenburg-Lindau, Germany. (marsch@mps.mpg.de)

S. Landi, L. Matteini, and M. Velli, Dipartimento di Astronomia e Scienza dello Spazio, Università degli Studi di Firenze, Largo E. Fermi 2, I-50125 Florence, Italy. (slandi@arcetri.astro.it; matteini@arcetri.astro.it; velli@arcetri.astro.it)